Synchrotron Radiation Small-Angle X-ray Scattering Study on the Deformation Mechanisms of a Toughened Nylon-6/ Poly(phenylene ether) Blend and High-Impact Polystyrene

Yasuhito Ijichi, Toshiro Kojima,† Yasuro Suzuki, Taichi Nishio,* and Masahiro Kakugo

Sumitomo Chemical Company, Ltd., Chiba Research Laboratory, 2-1 Kitasode, Sodegaura, Chiba, Japan

Yoshiyuki Amemiya

Photon Factory, National Laboratory for High Energy Physics, 1-1 Oho, Tsukuba, Ibaraki, Japan

Received December 30, 1991; Revised Manuscript Received October 26, 1992

ABSTRACT: Real-time measurements of the deformation processes of a nylon-6/poly(2,6-dimethyl-1,4-phenylene ether)/rubber blend (nylon/PPE/rubber blend) and high impact polystyrene (HIPS) were carried out by synchrotron radiation small-angle X-ray scattering (SR-SAXS). The specimens with 2-mm thickness were stretched at a speed of 0.5 mm/min, and the time-resolved scattering profiles were measured by imaging plate (IP) and position-sensitive proportional counter (PSPC). In the nylon/PPE/rubber blend, in which the matrix was nylon and PPE was the domain containing rubber inside with a relatively small particle diameter of about 0.2–0.5 μm, the voids began to form just before the yield point: The voids were initially almost isotropic and were deformed parallel to the tensile direction as elongation proceeded. It was found by transmission electron microscopy (TEM) that the voids formed at the rubber particles in the PPE domain. In HIPS with rubber particles of 4.9-μm average diameter, a diamondlike pattern was observed before the yield point, i.e., at a stress of about 84% of the yield stress. As the deformation proceeded beyond the yield point, a distinct perpendicular streak to the tensile direction arose and, therefore, the cross pattern was observed.

Introduction

Recently studies on the toughening mechanisms of polymer blends have attracted much attention from both the industrial and the scientific points of view. To this end, the deformation processes of polymer blends have been investigated by electron microscopy,[1] dilatometry,[2] X-ray scattering,[3,4] and recently synchrotron radiation small-angle X-ray scattering (SR-SAXS).[5–9] SR-SAXS is useful for dynamic analyses of the deformation processes because SR is extremely intense. Namely, the size and the volume of the voids formed in the range of 10 nm to a few hundred nanometers can be measured during the deformation.

Mills et al.[6] have examined crazes in polystyrene in a cyclic three-point bending test using SR-SAXS. They observed the intensity and the shape of the streak from the craze fibrils changed with the loading state. Further, they found that irreversible changes occurred in the pattern from one cycle to the next, which is due to craze growth, fibril breakdown, and permanent disorientation of fibrils.

Bubeck et al.[7] investigated crazes of high-impact polystyrene (HIPS) during tensile impact tests using SR-SAXS and showed a decrease in the craze volume with an increase in the deformation rate without significant changes in the craze microstructure. They investigated also poly(acrylonitrile–butadiene–styrene) (ABS) and a polycarbonate (PC)/ABS blend as well as HIPS, simultaneously measuring the absorption of the primary beam by the sample.[9] This technique made it possible to distinguish the strain due to crazing from that due to other deformation mechanisms, such as rubber particle cavitation and macroscopic shear deformation. They have demonstrated that crazing accounts for at most only half of the total plastic strain in HIPS and ABS and that in PC/ABS blends the predominant deformation mechanism is shear in the PC with associated rubber gel particle cavitation in the ABS.

The previous studies included analyses of crazes in styrenic polymers, polystyrene, HIPS, ABS,[8] and PC/ABS blends.[9]

In this study, we have applied SR-SAXS to the analysis of the cavitation process in a nylon/PPE/rubber blend. It has been found that the major energy-absorbing process in toughened nylon blends is the localized shear yielding associated with the cavitation of the rubber particles.[10] A nylon/PPE/rubber blend which has been recently developed is of industrial interest due to good impact resistance, good heat, and chemical stabilities.

Hobbs and Dekkers[2] investigated the deformation mechanism in a nylon/PPE/rubber blend using tensile dilatometry. They observed the cavitation of the dispersed rubber phase by scanning electron microscopy.

Sue and Yee[1] examined a nylon/PPE/rubber blend in a bending test. They showed by optical and electron microscopy that first a crazing zone was formed ahead of the crack tips and that it transformed into a shear yielding zone as the crack propagated.

In the present study, the deformation process of a nylon/PPE/rubber blend during a tensile test was first investigated by time-resolved analysis using SR-SAXS which gives dynamic and quantitative information on the size and volume of the voids. Transmission electron microscopy (TEM) was also used for the observation of deformed samples. In addition, HIPS was also investigated by SR-SAXS.

The deformation of the nylon/PPE/rubber blend was followed satisfactorily by SAXS which showed that the deformation proceeded with the void formation just before

† Tsukuba Research Laboratory, 6 Kitahara, Tsukuba, Ibaraki, Japan.

0024-9297/93/2226-0829$04.00/0

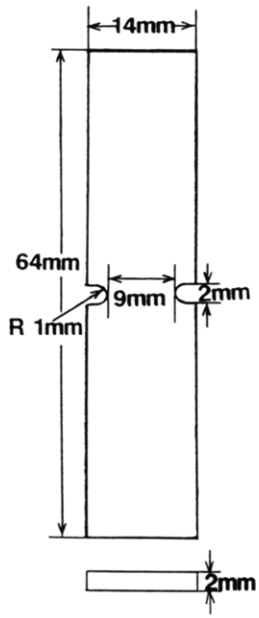

Figure 1. Schematic drawing of the tensile test specimen.

the yield point. The voids formed were initially isotropic and then deformed parallel to the tensile direction. The volume of the voids increased as the specimen was elongated. In HIPS with large-diameter (4.9 μm) rubber gel particles, craze began to form before the yield point, at a stress of about 84% of the yield stress, showing a diamondlike pattern. As the deformation proceeded beyond the yield point, a cross pattern was observed due to the distinct perpendicular streak caused by the stretched fibrils within the craze.

Experimental Section

Samples. Nylon-6 with a number-average molecular weight ($\bar{M}_n$) of 21 000 was used. The $\bar{M}_n$ of poly(2,6-dimethyl-1,4-phenylene ether) (PPE) was 19 000. The rubber was a styrene-hydrogenated-butadiene-styrene triblock copolymer (SEBS), and the molecular weight of each end block (polystyrene) was 29 000 and that of the midblock was 116 000. The composition of the blend was 41.6 wt % of nylon, 38.4% wt % of PPE, and 20 wt % of rubber. The nylon/PPE/rubber blend was prepared by compounding each component and a coupling agent of nylon and PPE in a twin screw extruder. The HIPS contained 6.8 wt % of polybutadiene. The weight-average molecular weight of polystyrene was 310 000.

Tensile specimens cut from compression-molded sheets were 64 mm long, 14 mm wide, and 2 mm thick. Two U-notches with a radius of 1.0 mm were machined as stress concentrators in both sides of the middle of the specimens as shown in Figure 1. The distance of the tips of the notches was 9 mm. Stress was calculated on the basis of the cross-sectional area of 9 mm × 2 mm between two notch tips.

Apparatus. The tensile tests were performed with a specially designed tensile instrument. Two fixtures move in opposite directions at the same speed so that the center of the specimen is always held at the direct beam position. The test speed was 0.5 mm/min. The span of the two fixtures was 50 mm.

SAXS measurement was performed at the National Laboratory for High Energy Physics (Japan) using the facilities BL-15A[11] at the Photon Factory. The collimation system in the line was a curved mirror and a curved monochromator. The wavelength of monochromatized X-rays was 0.150 nm. An imaging plate (IP) was used for two-dimensional measurements at several points during the course of each tensile test to detect the change of SAXS patterns.[12] The sampling unit time of IP was 0.1 s. A position-sensitive proportional counter (PSPC) was also used for time-resolved SAXS measurements for quantitative analyses. The sampling unit time of PSPC was 10 s for a nylon/PPE/rubber blend and 5 s for HIPS. Quantitative measurements of scattering intensities in parallel and perpendicular directions to the tensile axis were carried out for two different test specimens with PSPC.

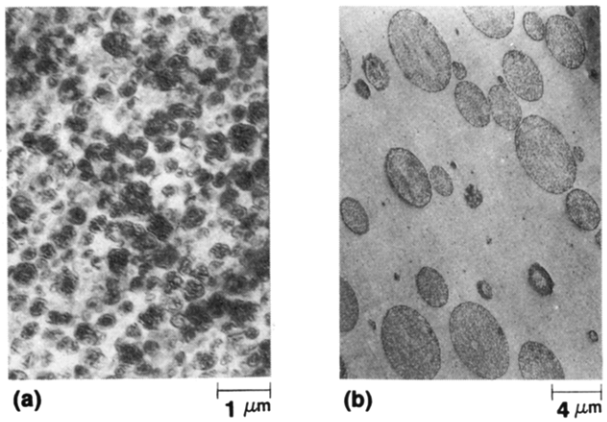

Figure 2. TEM micrographs of undeformed samples. (a) Nylon/PPE/rubber blend. Polystyrene blocks in the rubber (SEBS) were stained darkly, and the PPE was stained palely. (b) HIPS. Polybutadiene was stained.

Electron Microscopy. The specimen of HIPS was stained with a 4% aqueous solution of osmium tetroxide for 3 h at 60 °C and then microtomed using a Reichert Ultracut N ultramicrotome. Thin sections of a nylon/PPE/rubber blend were stained with a 1% aqueous solution of ruthenium tetroxide for several seconds at room temperature. The thin sections were examined with a Hitachi H-8000 TEM.

Results and Discussion

I. Real-Time SR-SAXS Measurements of a Nylon/PPE/Rubber Blend and HIPS during Deformation. Morphologies of the Samples. The morphologies of nylon/PPE/rubber and HIPS were observed by TEM. Figure 2a shows an electron micrograph of the nylon/PPE/rubber blend in which a fine PPE domain (ca. 0.2–0.5 μm) containing rubber (ca. 0.1–0.4 μm) inside was dispersed in the matrix of nylon. Figure 2b shows an electron micrograph of HIPS in which rubber particles with polystyrene inclusions were 4.9 μm in average diameter.

Two-Dimensional SAXS Patterns. Two-dimensional SAXS patterns of the nylon/PPE/rubber blend during a tensile test were measured with IP and shown in Figure 3 together with the stress–strain curve. In the elastic deformation region, pattern (A) was the same as the undeformed SAXS pattern (isotropic). At the point slightly exceeding the yield point, pattern (B) increased in intensity and, however, was still nearly isotropic. Pattern (C) further elongated beyond the yield point became anisotropic, perpendicular to the tensile direction. This indicates that the isotropic voids which began to form near the yield point deformed parallel to the tensile direction as the elongation further proceeded.

Figure 4 shows the SAXS patterns and the stress–strain curve of HIPS. In the elastic deformation region, HIPS also showed an isotropic pattern (A). Just before the yield point, SAXS pattern (B) first showed a diamondlike pattern having a streak parallel to the tensile direction resulting from the external reflection of the interfaces of the crazes with bulk polymer. When the specimen was further stretched (the SAXS pattern (C)), the distinct streak perpendicular to the tensile direction arose, showing a cross pattern. In the cross pattern,[4-9] the perpendicular streak is caused by stretched fibrils parallel to the tensile direction within the craze.

Time-Resolved SAXS Measurement. The time-resolved scattering intensities were measured with PSPC. Figure 5 shows parallel and perpendicular SAXS profiles

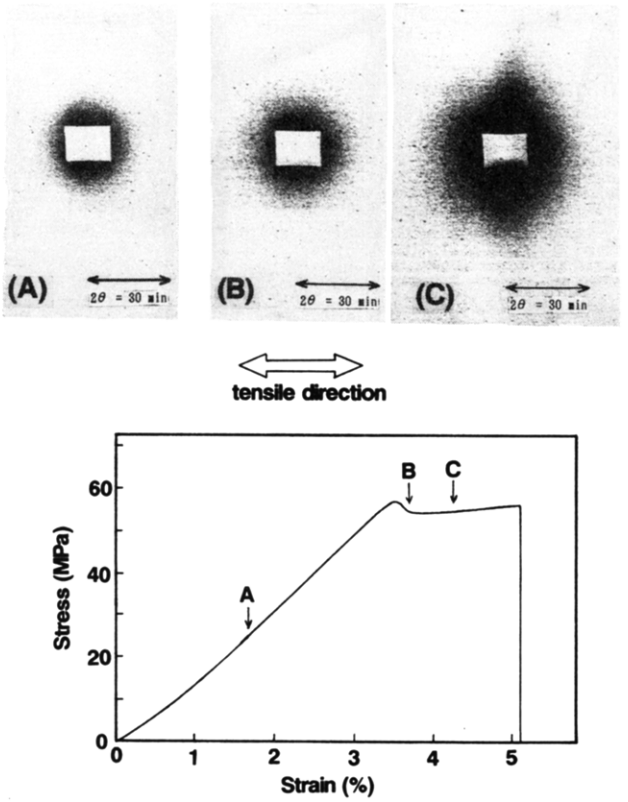

Figure 3. SAXS patterns and stress–strain curve of a nylon/PPE/rubber blend during a tensile test. The tensile direction is horizontal. The SAXS patterns (A)–(C) were measured at points A–C on the stress–strain curve.

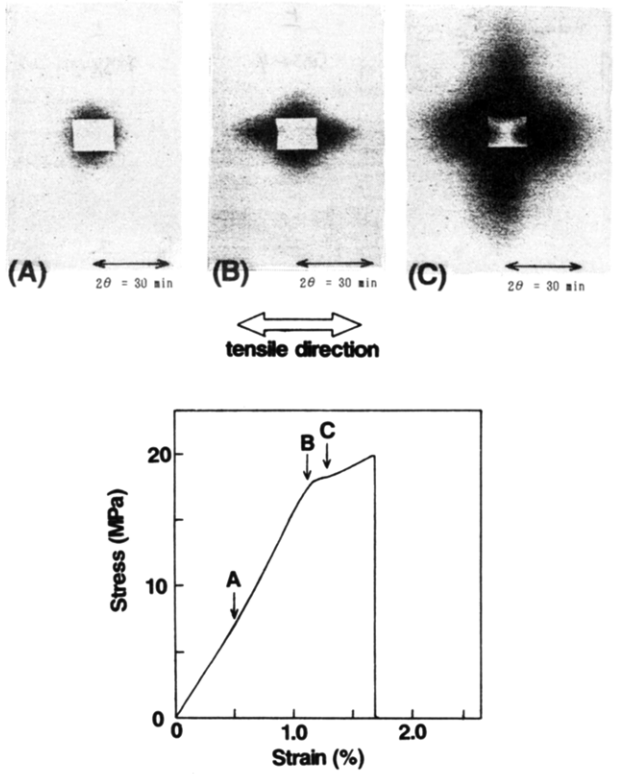

Figure 4. SAXS patterns and stress–strain curve of HIPS during a tensile test. The tensile direction is horizontal. The SAXS patterns (A)–(C) were measured at points A–C on the stress–strain curve.

of the nylon/PPE/rubber blend during tensile tests in which no peaks were observed. The perpendicular profiles in Figure 5b increased in intensity monotonously with an

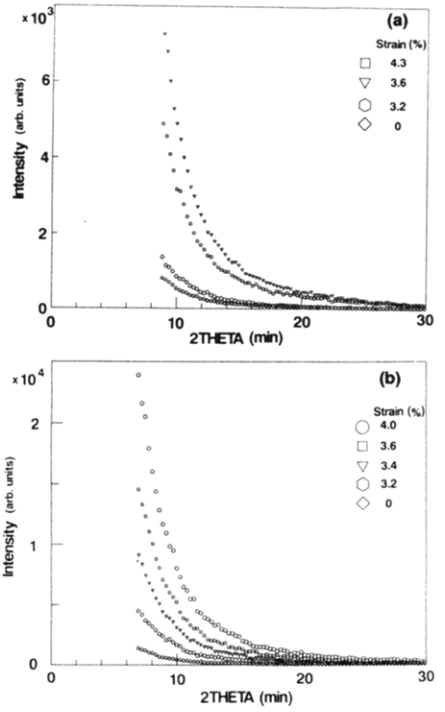

Figure 5. Scattering profiles of a nylon/PPE/rubber blend. (a) Parallel to the tensile direction. (b) Perpendicular to the tensile direction. Each profile was taken at the indicated strain level.

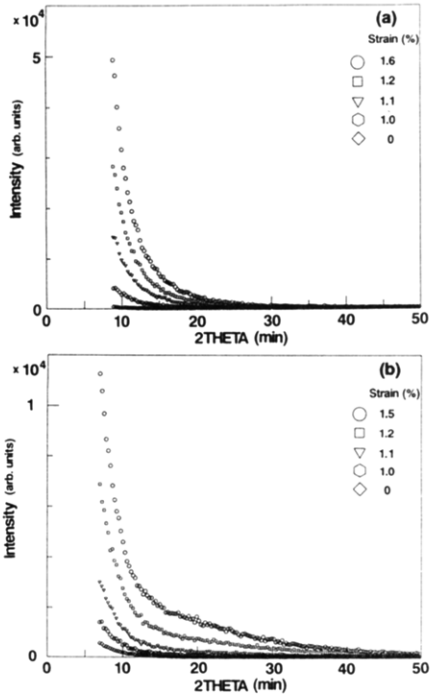

Figure 6. Scattering profiles of HIPS. (a) Parallel to the tensile direction. (b) Perpendicular to the tensile direction. Each profile was taken at the indicated strain level.

increase in elongation, whereas the parallel profiles in Figure 5a increased up to 3.6% strain and decreased beyond this point due to a growth of voids beyond the resolution of the apparatus.

Figure 6 shows SAXS profiles of HIPS in which no peaks were observed. Both parallel and perpendicular profiles in parts a and b of Figure 6 increased in intensity with an increase in elongation. The scattering intensity of the parallel profiles was higher than that of the perpendicular profiles in a low-angle region. On the other hand, in a high-angle region, the perpendicular profiles showed higher

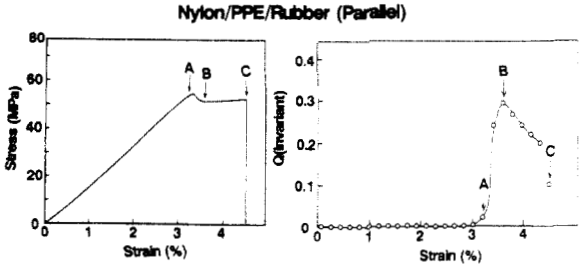

Figure 7. Stress–strain and invariant Q value curves of a nylon/PPE/rubber blend parallel to the tensile direction. The points A–C in the stress–strain curve correspond to those in the Q change curve.

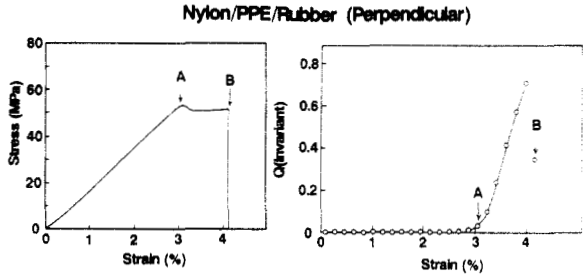

Figure 8. Stress–strain and invariant Q value curves of a nylon/PPE/rubber blend perpendicular to the tensile direction. The points A and B in the stress–strain curve correspond to those in the Q change curve.

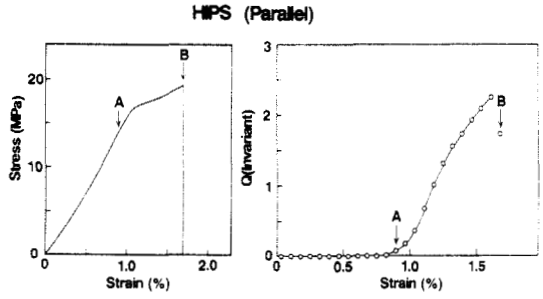

Figure 9. Stress–strain and invariant Q value curves of HIPS parallel to the tensile direction. Points A and B in the stress–strain curve correspond to those in the Q change curve.

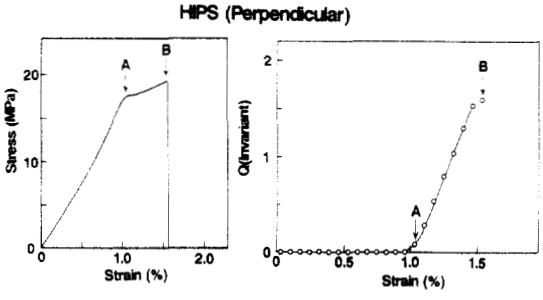

Figure 10. Stress–strain and invariant Q value curve of HIPS perpendicular to the tensile direction. Points A and B in the stress–strain curve correspond to those in the Q change curve.

intensities than the corresponding parallel profiles. This is known to be due to the fibrils parallel to the tensile direction.

II. Q Value Analyses of a Nylon/PPE/Rubber Blend and HIPS. X-ray scattering intensity is proportional to the square of the electron density difference between two phases. The electron densities of the polymers used in this study range from 0.49 mol of electron/cm^3 for polybutadiene to 0.63 mol of electron/cm^3 for nylon-6. On the other hand, if the voids were filled with air, the electron density of the voids is 0.0012 mol of electron/cm^3 which is 2 orders of magnitude lower than those of the polymers. Therefore, the voids contribute mostly to the scattering.

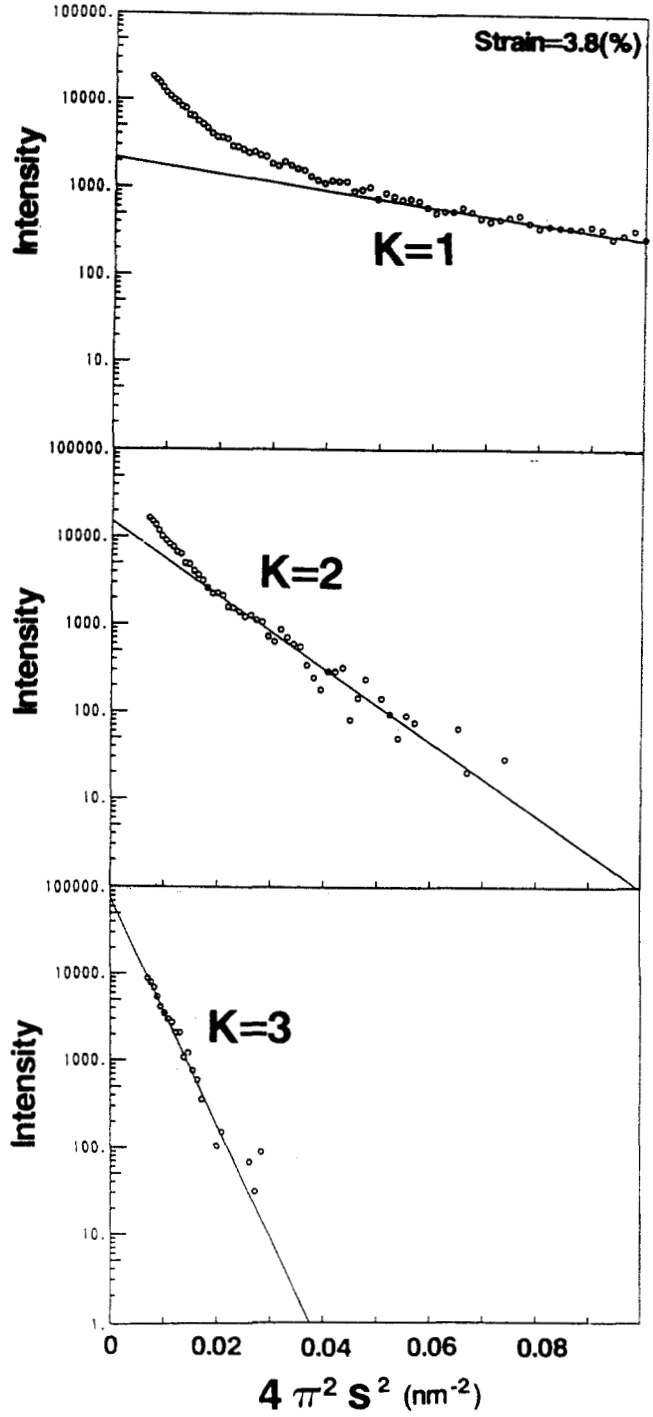

Figure 11. Guinier plots of the scattering profile of a nylon/PPE/rubber blend perpendicular to the tensile direction at 3.8% strain.

The small-angle scattering invariant allows us to estimate the quantity of the formed voids. The invariant Q is defined as

$$Q = 4\pi \int_0^\infty I(s)\, s^2\, ds$$
$$= C(\rho_1 - \rho_2)^2 \phi(1-\phi) \qquad (1)$$

where s is the magnitude of the scattering vector defined as $2(\sin\theta)/\lambda$, 2θ is the scattering angle, λ is the wavelength of the X-rays, ρ_1 is the electron density of the polymer, ρ_2 is that of the voids, ϕ is the volume fraction of the voids, and C is a constant. A background scattering intensity, measured from the undeformed sample, was subtracted

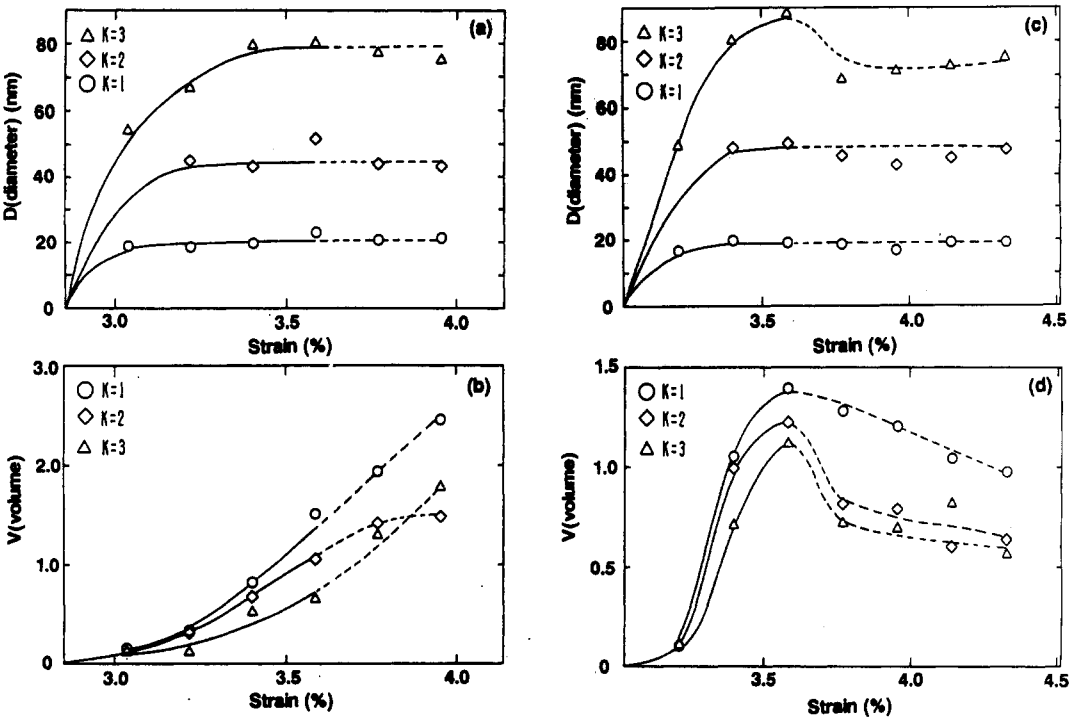

Figure 12. Sizes and volumes of the voids in a nylon/PPE/rubber blend. In the perpendicular direction to the tensile axis: (a) change of the diameter of the voids; (b) change of the relative volume of the voids. In the parallel direction to the tensile axis: (c) change of the diameter of the voids; (d) change of the relative volume of the voids.

from the scattering intensity of the deformed samples, neglecting the volume change of the sample during deformation.

Figure 7 shows a Q value curve parallel to the tensile direction of the nylon/PPE/rubber blend with the corresponding stress–strain curve. In the elastic deformation region, the Q value showed no change, indicating no void formation. In the region close to the yield point, the Q value increased remarkably. This shows clearly that the voids formed just before the yield point and drastically increased beyond the point. As the deformation proceeded further, the Q value, however, decreased inversely. On the other hand, the Q value curve perpendicular to the tensile direction shown in Figure 8 increased monotonously until the break. This difference indicates that the voids were stretched predominantly parallel to the tensile direction.

Figure 9 shows a Q value curve of HIPS parallel to the tensile direction with the corresponding stress–strain curve. The Q value began to increase before the yield point. The stress of point A in Figure 9 was 13.9 MPa which was 16% lower than the yield stress, 16.5 MPa. Figure 10 shows a Q value curve of HIPS perpendicular to the tensile direction. The Q value began to increase just before the yield point resulting from the stretched fibrils within crazes.

III. Guinier Analysis of a Nylon/PPE/Rubber Blend. On HIPS or a polystyrene system, many studies have been made with SAXS to estimate the amount of craze volume, fibril diameter, and several other parameters using Porod analysis[3-9] and other methods.[13] On the other hand, SAXS has been seldom applied to the deformation processes of voids forming polymer systems.[9]

From now on, we focus on the deformation process of a nylon/PPE/rubber blend and concentrate to investigate it in detail.

Analysis of the Size and Volume of the Voids. To analyze the size and volume of the formed voids, we adopted a Guinier approximation which is valid only for a system with no interparticle interference. For a system with a particle size distribution, the generalized Guinier approximation[14] is applicable and is expressed as

$$I(s) = C\sum_i N_i V_i^2 \exp(-\pi^2 D_i^2 s^2/5) \qquad (2)$$

where D_i is the diameter of the particles, N_i is the number and V_i is the volume of the particles with diameter D_i, and C is a constant. In the present case particles mean voids. In the case of crazes, the voids within the crazes have regular arrangements. As described above, HIPS showed the anisotropic pattern (Figure 4) resulting from the formation of crazes that most likely caused interparticle interference. Therefore, Guinier analysis is inapplicable to HIPS. On the other hand, a nylon/PPE/rubber blend showed almost isotropic patterns (Figure 3), and no crazes were shown in Figure 13. In this case Guinier analysis can be applied. Figure 11 shows the Guinier plots for the nylon/PPE/rubber blend in which the scattering curve of the undeformed state was subtracted from the scattering curves of the deformed sample as a background. In consideration of analytical accuracy, the voids were divided into three size groups which substituted for a continuous distribution of void size. K number denotes the size group; 1–3 correspond to the smallest to the largest.

Parts a and b of Figure 12 show the analytical results of the perpendicular profiles. In Figure 12a, the sizes of the voids are plotted against strain. The void sizes increased and approached the individual constant values, about 20, 40, and 80 nm. The reason for the largest void size reaching the constant value is probably because the voids which grew up beyond the resolution of the SAXS apparatus were unable to be detected. In Figure 12b, each volume of the voids increased with an increase in elongation, which indicates the voids formed continuously with elongation.

Parts c and d of Figure 12 show the analytical results of the parallel profiles. In Figure 12c, all the void sizes increased at first, and the small (K = 1) and middle (K

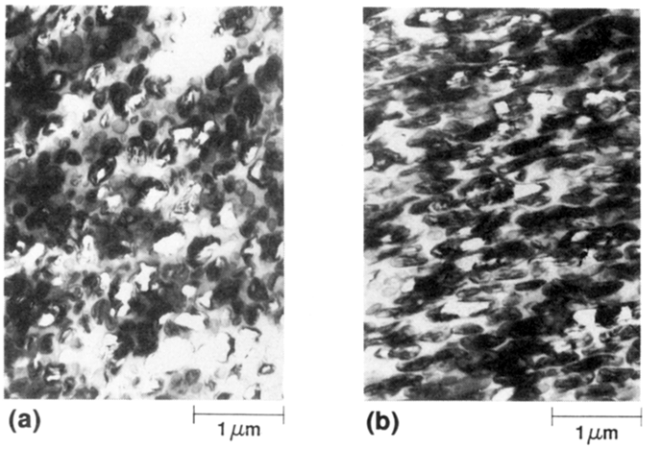

Figure 13. TEM micrographs of a nylon/PPE/rubber blend at the break. (a) The micrograph of the thin section perpendicular to the tensile direction. (b) The micrograph of the thin section parallel to the tensile direction. Polystyrene of the rubber (SEBS) was stained darkly, and PPE was stained palely with RuO_4.

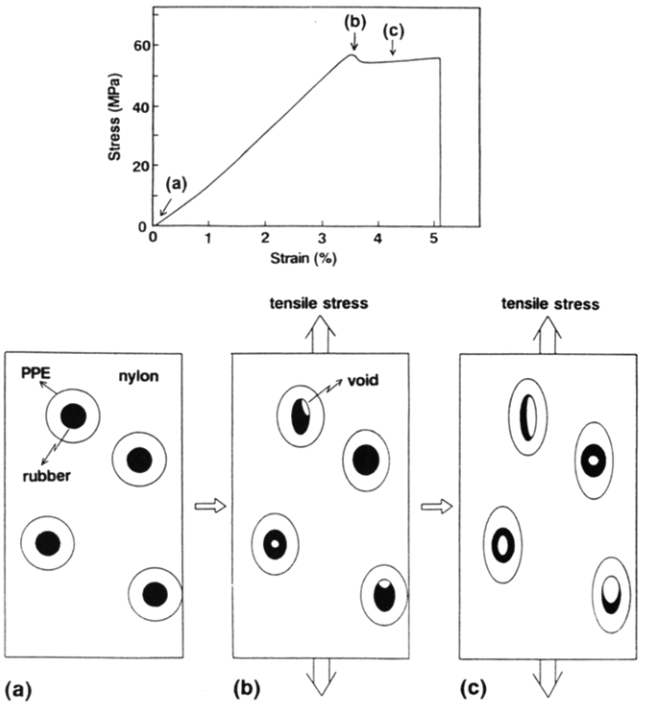

Figure 14. Schematic deformation model and stress–strain curve of a nylon/PPE/rubber blend. (a) Undeformed state. (b and c) Voids generate successively with elongation and are deformed parallel to the tensile direction.

= 2) void sizes also approached the individual constant values, about 20 and 40 nm. However, the largest void size showed a little decrease beyond 3.6% strain. In Figure 12d, the volume of each size voids increased until 3.6% strain where the Q value showed the maximum, however, beyond this point, decreased gradually.

One of the reasons for the apparent decrease in the void volume in parts b and d of Figure 12 was the decrease in irradiated volume caused by sample thinning during the deformation, which decreased the scattering intensity equally in both parallel and perpendicular directions. On the condition that the voids are isotropic, the size and volume of the voids change in the same way in both parallel and perpendicular directions. Beyond 3.6% elongation, there can be the difference in the size of the voids in the parallel and perpendicular directions which means that the voids were elongated in the parallel direction. Therefore, Guinier analytical data show no significant meaning beyond 3.6% elongation.

TEM micrographs of the specimen at the break of the nylon/PPE/rubber blend are shown in Figure 13.

In the perpendicular direction, in Figure 13a, the PPE domain containing the rubber was seldom deformed. Voids appeared to form at the rubber particles in the PPE domain.

In the parallel direction, in Figure 13b, the PPE domain and the voids within them were elongated substantially in the tensile direction. Some voids formed in the rubber, and other voids formed at the interface between the rubber and the PPE. No voids were observed at the interface between the PPE and the nylon, and no crazes were observed.

Deformation Mechanism. In the present study, the deformation processes were observed during tensile tests. On the basis of the results obtained by SR-SAXS and TEM, the deformation mechanism of the nylon/PPE/rubber blend is discussed.

When tensile stress was applied to a test specimen, the rubber particles acted as stress concentrators at first, and just before the yield point, voids formed at the rubber particles in the PPE domain. In this initial stage, the formed voids were isotropic. These voids had a role of relieving the hydrostatic pressure of a nylon/PPE matrix.

Analyses of the SAXS profiles showed voids had a size distribution. With an increase in strain, the volume of each size void in the perpendicular direction monotonously increased, which indicates the voids successively generated and stably grow up. As the deformation of the specimen further proceeded, the voids deformed parallel to the tensile direction. During the growth of these voids, much of the shear yielding enhanced by the presence of the voids was taking place, which led to a lot of energy dissipation of the blend.

From the Guinier analytical data and the TEM micrographs, a schematic deformation model of a nylon/PPE/rubber blend is illustrated in Figure 14.

Conclusions

Real-time SAXS measurements of a nylon/PPE/rubber blend and HIPS were performed during tensile tests using SR. In addition, TEM observation of the nylon/PPE/rubber blend was carried out.

(1) SR-SAXS is demonstrated to be useful for the study of polymer deformation processes involving voids as well as craze because it provides real-time as well as quantitative information.

(2) In the nylon/PPE/rubber blend, voids began to form just before the yield point at the rubber particles in the PPE domain. The voids were initially almost isotropic and deformed parallel to the tensile direction with an increase in elongation.

(3) In HIPS, a diamondlike SAXS pattern was first observed at the stress lower than the yield stress. Beyond the yield point, a cross pattern was observed due to the distinct perpendicular streak caused by the stretched fibrils within crazes.

References and Notes

(1) Sue, H. J.; Yee, A. F. *J. Mater. Sci.* **1989**, *24*, 1447.
(2) Hobbs, S. Y.; Dekkers, M. E. J. *J. Mater. Sci.* **1989**, *24*, 1316.
(3) Steger, T. R.; Nielsen, L. E. *J. Polym. Sci., Polym. Phys. Ed.* **1978**, *16*, 613.
(4) Brown, H. R.; Kramer, E. J. *J. Macromol. Sci., Phys.* **1981**, *B19* (3), 487.
(5) Brown, H. R.; Mills, P. J.; Kramer, E. J. *J. Polym. Sci., Polym. Phys. Ed.* **1985**, *23*, 1857.

(6) Mills, P. J.; Kramer, E. J.; Brown, H. R. *J. Mater. Sci.* **1985**, *20*, 4413.
(7) Bubeck, R. A.; Blazy, J. A.; Kramer, E. J.; Buckley, D. J.; Brown, H. R. *Polym. Commun.* **1986**, *27*, 357.
(8) Bubeck, R. A.; Blazy, J. A.; Kramer, E. J.; Buckley, D. J.; Brown, H. R. *Mater. Res. Soc. Symp. Proc.* **1987**, *79*, 293.
(9) Bubeck, R. A.; Buckley, D. J., Jr.; Kramer, E. J.; Brown, H. R. *J. Mater. Sci.* **1991**, *26*, 6249.
(10) Borggreve, R. J. M.; Gaymans, R. J.; Eichenwald, H. M. *Polymer* **1989**, *30*, 78.
(11) Amemiya, Y.; Wakabayashi, K.; Hamanaka, T.; Wakabayashi, T.; Matsushita, T.; Hashizume, H. *Nucl. Instrum. Method* **1983**, *208*, 471.
(12) Amemiya, Y.; Matsushita, T.; Nakagawa, A.; Satow, Y.; Miyahara, J.; Chikawa, J. *Nucl. Instrum. Method Phys. Res.* **1988**, *A266*, 645.
(13) Westbrook, P. A.; Fellers, J. F.; Hendricks, R. W.; Lin, J. S. *J. Polym. Sci., Polym. Phys. Ed.* **1983**, *21*, 969.
(14) Klug, H. P.; Alexander, L. E. *X-Ray Diffraction Procedures*; John Wiley & Sons: New York, 1959; p 661.